

Benign Yellow Dot Maculopathy - a new macular phenotype

Arundhati Dev Borman^{1,2}, Aleksandra Rachitskaya³, Martina Suzani¹, Robert A. Sisk⁴, Zubair M. Ahmed⁵, Graham E. Holder¹, Valentina Cipriani^{1,2,6}, Gavin Arno^{1,2}, Andrew R. Webster^{1,2}, Robert B. Hufnagel⁷, Audina Berrocal³, Anthony T. Moore^{1,2,8}

Affiliations

1. Moorfields Eye Hospital NHS Foundation Trust, London, UK
2. UCL Institute of Ophthalmology, London, UK
3. Bascom Palmer Eye Institute, University of Miami Miller School of Medicine, Miami, FL, USA
4. Cincinnati Eye Institute, Cincinnati, OH, USA, University of Cincinnati Department of Ophthalmology, Abrahamson Pediatric Eye Institute, Cincinnati Children's Hospital, Cincinnati, OH, USA
5. Otorhinolaryngology Head & Neck Surgery, University of Maryland School of Medicine, Baltimore, MD, USA
6. UCL Genetics Institute, London, UK
7. Ophthalmic Genetics and Visual Function Branch, National Eye Institute, National Institutes of Health, Bethesda, MD, USA
8. Ophthalmology Department, University of California San Francisco, CA, USA

Corresponding Author and Address for Reprints

Arundhati Dev Borman MD(Res) FRCOphth

Genetics Office, Professorial Unit

Moorfields Eye Hospital, 132 City Road

London EC1V 2PD, UK

Email: a.dev-borman@ucl.ac.uk

Financial Disclosures

None

Conflict of Interest

No conflicting relationship exists for any author

Acknowledgements

We thank Moshin Shazad for help with linkage data. The authors are grateful for support from the National Institute for Health Research Biomedical Research Centre at Moorfields Eye Hospital NHS Foundation Trust and UCL Institute of Ophthalmology (UK), Fight for Sight, Foundation Fighting Blindness (USA) and Research to Prevent Blindness (USA). The views expressed in this publication are those of the authors and not necessarily those of the Department of Health.

Running Head

Benign Yellow Dot Maculopathy

Abstract

Objective

To describe a novel macular phenotype that is associated with normal visual function.

Design

Retrospective observational case series.

Participants

36 affected individuals from 23 unrelated families.

Methods

This was a retrospective study of patients who had a characteristic macular phenotype. Subjects underwent a full ocular examination, electrophysiological studies, spectral domain optical coherence tomography (OCT) and fundus autofluorescence imaging. Genomic analyses were performed using haplotype sharing analysis and whole-exome sequencing.

Main Outcome Measures

Visual acuity; Retinal features; Electroretinography; Whole-exome sequencing; Haplotype sharing analysis.

Results

Twenty-six of 36 subjects were female. The median age at presentation was 15 years, range 5-59 years. The majority of subjects were asymptomatic and either presented following a routine eye examination (22/36 subjects), following screening due to a positive family history (13/36 subjects) or from another ophthalmologist (1/36 subjects). Of the three symptomatic subjects, 2 had reduced visual acuity. Reduced vision was attributed to diagnoses of non-organic visual loss and bilateral ametropic amblyopia with strabismus. Visual acuity was 0.18 LogMAR or better in 30/33 subjects. Color vision was normal in all subjects tested, except for the subject with non-organic visual loss.

All subjects had bilateral symmetric multiple yellow dots at the macula. In the majority these were evenly distributed throughout the fovea, but in nine subjects they were concentrated in the nasal parafoveal area. The dots were hyperautofluorescent on fundus autofluorescence imaging. OCT imaging was generally normal, but in 6 subjects subtle irregularities at the inner segment ellipsoid band were seen. Electrophysiological studies identified normal macular function in 17/19 subjects and normal full-field retinal function in all subjects. Whole-exome analysis across 3 unrelated families found no pathogenic variants in known macular dystrophy genes. Haplotype sharing analysis in one family excluded linkage with the North Carolina macular dystrophy (MCDR1) locus.

Conclusions

A new retinal phenotype is described, which is characterised by bilateral multiple early onset yellow dots at the macula. Visual function is normal and the condition is non-progressive. In familial cases, the phenotype appears to be inherited in an autosomal dominant manner, but a causative gene is yet to be ascertained.

Introduction

The inherited macular dystrophies are a clinically and genetically heterogeneous group of disorders in which there are structural and functional abnormalities of the central retina [1], [2]. These disorders usually occur in isolation, but they may be associated with a variety of systemic abnormalities. All of the Mendelian and mitochondrial inheritance patterns have been described [3]. Most forms of macular dystrophy present in later childhood or in adult life after a period of normal visual development, and are usually progressive. The exception is a rare group of disorders that present with visual impairment in infancy and where there is abnormal foveal or macular development [4]. Such disorders do not commonly progress.

Although most macular dystrophies present with central visual loss, some patients with normal visual acuity are referred to ophthalmologists when a macular abnormality is noted on routine optometric examination. Whatever the mode of presentation, the specific diagnosis is made on the basis of the macular appearance, along with retinal imaging, electrophysiological studies, inheritance patterns and, increasingly, the results of molecular genetic testing [5]. Some clinical phenotypes do not easily fit into well-characterised disorders.

The present report describes a novel macular phenotype that may occur in isolation, or as a familial trait, which is non-progressive, and which is associated with normal visual function.

Methods

Subjects

Subjects were ascertained based upon the presence of a specific macular phenotype, and were recruited from the pediatric and adult medical retina clinics of three ophthalmologists (one UK, two USA). Informed consent was obtained from all subjects and family members involved in this study. The study had IRB approval from Cincinnati Children's Hospital, Bascom Palmer Eye Hospital and the Moorfields Eye Hospital Local Research Ethics Committee, and all investigations were conducted in accordance with the principles of the Declaration of Helsinki.

Clinical Examination

Best-corrected monocular visual acuity (VA) was measured using a logMAR scale and color vision was assessed using Ishihara pseudoisochromatic plates, Hardy Rand Rittler (HRR) color plates and the Farnsworth-Munsell 100 Hue Test. Funduscopy and slit-lamp biomicroscopy were performed. Color fundus photography was undertaken in all subjects; in the majority this was carried out using a Topcon TRC 501A retinal camera (Topcon Corporation, Tokyo, Japan), but in some individuals, seen early in the study period, a Zeiss retinal film camera was used. Spectral domain optical coherence tomography (sd-OCT) using a Heidelberg SPECTRALIS® Spectral domain OCT scanner (Heidelberg Engineering, Dossenheim, Germany) and fundus autofluorescence (FAF) imaging (Heidelberg Engineering, Dossenheim, Germany) were also performed. Electrophysiological assessment including full-field electroretinography (ERG), pattern electroretinography (PERG) and Electro-Oculograms (EOG) were performed in the subjects from the UK according to the recommendations of the International Society for Clinical Electrophysiology of Vision (ISCEV) [6]-[7, 8]. Fundus fluorescein angiography was also undertaken in selected subjects.

Genomic analyses

DNA was extracted from whole blood by standard methods. Whole-exome sequencing (WES) was performed for Family 4 (Subjects 8, 9, 11), Moorfields Eye Hospital Genetic Clinic (GC)

number GC14302, Family 8 (Subjects 19, 20, 21) and Family 22 (Subject 35), as previously described [9]. Briefly, dsDNA was sheared by sonication to an average size of 200 bp. After nine cycles of PCR amplification using the Clontech Advantage II kit, 1 µg of genomic library was recovered for exome enrichment using the NimbleGen EZ Exome V2 kit. Libraries were sequenced on an Illumina HiSeq2500. Data analysis used the Broad Institute's Genome Analysis Toolkit (GATK) [10]. Reads were aligned with the Illumina Chastity Filter with the Burrows Wheeler Aligner [11]. Variant sites were called using the GATK UnifiedGenotyper module [10]. Variant filtering and group analysis was performed using Qiagen Ingenuity Variant Analysis.

Haplotype sharing analysis was performed on SNP data from 5 affected members of Family 4 genotyped using the Illumina HumanOmniExpress-24 v1.0 beadchip (Illumina, Inc., San Diego, CA, USA) that includes over 715,000 SNPs. Genotypes were determined using the Genotyping Module in the Illumina GenomeStudio v2011.1 software. Build hg19/GRCh37 was used to annotate chromosomal coordinates. The haplotype sharing analysis was carried out using the non-parametric Homozygosity Haplotype (HH) method that searches for chromosomal segments sharing the same haplotype across affected individuals (as an indication of genetic linkage with the disease) [12]. The HH is a type of haplotype described by the homozygous SNPs only (all heterozygous SNPs are removed). Since affected family members who inherited the same mutation from a common ancestor share a chromosomal segment identical-by-descent (IBD) around the disease gene, they should not have discordant homozygous calls in the IBD region and thus they should share the same HH. The HH approach predicts IBD regions through the identification of regions with a conserved HH (RCHHs) defined as those regions with a shared HH among patients and a genetic length longer than a certain cut-off value (recommended cut-off for Illumina array is 2.5/3.0 cM).

Results

Thirty-six affected individuals were identified from 23 unrelated families. Subjects were either referred from community optometrists (22/36), from another ophthalmologist (1/36) or following screening due to a positive family history (13/36). Of the 36 subjects, 15 were sporadic. Twelve of the 15 sporadic cases were Caucasian, 1 was of West African origin, 1 of South Asian descent, and 1 of African-Caribbean descent. Eight families (all Caucasian) demonstrated an autosomal dominant inheritance pattern (Figure 1, pedigree of Family 4). The median age at presentation was 15 years, range 5-59 years. Twenty-six of 36 subjects were female (Table 1).

Thirty-three subjects (91.7%) were asymptomatic. One subject complained of floaters (Subject 35) but had normal visual acuities and a normal peripheral retinal examination. Reduced visual acuity was the presenting complaint in the other two symptomatic subjects (Subjects 8 and 23). No cause was found for the reduced vision in Subject 8, who presented at age 16 years, and in whom multiple electrophysiological studies over a number of years were normal. A diagnosis of 'non-organic' visual loss was made. Subject 23 presented to another ophthalmologist at age 4 years with reduced vision, attributed to bilateral ametropic amblyopia due to hypermetropic astigmatism; macular yellow dots were not identified until age 6 years. His vision eventually improved with refractive correction and occlusion therapy to 0.18 OD and 0.26 OS.

Refractive error (identified in 15 subjects) was the predominant finding in the 17 subjects who had any past ocular history (Table 1). Two of 17 had been treated for strabismus and 3/17 had been treated for amblyopia. One subject developed bilateral optic neuropathy of unknown etiology, during the follow-up period, four and a half years after presentation with the macular phenotype, which resolved spontaneously; and one had non-organic visual loss. General health was good in all, except for Subject 33, who was taking antidepressants.

Visual acuity (VA) at presentation was 0.18 LogMAR or better in both eyes in 30/33 subjects (Table 1). In 3 subjects the VA was unrecorded (these were all affected family members of probands). Subject 8, with non-organic visual loss, had a presenting VA of 0.78 LogMAR in either eye. Amblyopia affected Subjects 23 (bilateral), 27 (unilateral right eye) and 28 (unilateral left eye) (Table 1). Successful amblyopia therapy improved the acuity in Subject 28 to better than 0.18 LogMAR OU. The finding of amblyopia and refractive error in a subset of patients likely reflects the fact that the majority of subjects were ascertained in ophthalmology or optometry clinics. Color vision was normal in 23 of 24 subjects examined, using a variety of color vision tests. Only one subject had mild colour vision abnormalities (Subject 8). She failed two of the HRR screening plates at age 16 years. Anterior segments and ocular mediae were normal in all subjects.

Funduscopy in all subjects revealed characteristic bilateral macular changes consisting of yellow dots at the level of the retinal pigment epithelium (RPE), concentrated around the fovea. These were symmetrical between each eye in all subjects (Figure 2). In the majority of subjects the dots were fine and discrete but in 9 subjects some of the dots were confluent (Table 2). The yellow dots were distributed evenly around the fovea in 13 subjects; in 10 they were concentrated in the nasal parafoveal region. In Subjects 22 and 24 a few additional dots were visible outside the temporal vascular arcades in the right eye. In all but 1 subject (Subject 23) where detailed images were available (26/36), a yellow crescent was visible to varying degrees around the optic disc, which was otherwise normal in all (Table 2, Figure 2). The retinal periphery and vasculature were otherwise normal in all subjects. Funduscopy was normal in all parents of the sporadic cases that were examined.

Fundus autofluorescence imaging, available for 22/36 subjects, revealed foci of hyperautofluorescence corresponding to the yellow dots on otherwise normal background autofluorescence (Figure 3). The autofluorescence imaging did not reveal any lesions other than those visible on funduscopy.

Sd-OCT imaging was performed in 18 subjects and was normal in 11. There was minimal irregularity of the inner segment ellipsoid (ISE) band in 6 subjects (Subjects 11, 14, 16, 17, 23, 26), corresponding to the locations of the yellow dots, as observed on the infrared reflectance image (Figure 4). In one additional subject the only change seen on OCT imaging was a mild irregularity of the RPE layer (Subject 28).

Electroretinography was performed in 19 subjects. The ERG was normal in all 19 subjects, and the PERG was abnormal in 2. There was a mildly subnormal PERG P50 component amplitude in subject 4. In Subject 28 the PERG was moderately subnormal in each eye, indicative of moderate macular dysfunction. EOGs in 9 of 10 subjects demonstrated a normal light rise. In Subject 28 the EOG was of poor technical quality, which precluded accurate quantification of the light rise.

Fundus fluorescein angiography performed in 3 subjects (Subjects 2, 14 and 17) demonstrated early hyperfluorescence of the dots with no change in size or intensity over time.

WES was performed in affected members of Family 4, Family 8 and Family 22. After filtering for retinal dystrophy-associated genes and genes within the MCDR1 locus on chromosome 6 and MCDR3 locus on chromosome 5, no rare variants were found to consistently segregate with the macular phenotype in any of the known retinal disease genes. Additionally, gene-level analysis did not detect exonic or splice site variants in the same gene for two or more families. Therefore, non-coding causes were predicted as a common mechanism, as has been reported for MCDR1 and MCDR3 [13, 14]. Genome-wide analysis was performed for family 4 using SNP chips. A search for a shared IBD chromosomal segment among the five affected individuals with SNP chip data in family 4 (GC14302) was performed using the HH method. The haplotype sharing analysis revealed no evidence of linkage at the MCDR1 locus (Supplementary Table 1 and Supplementary Figure 1). There were 10 regions (on chromosome 2, 3, 5, 6, 8, 11, 17, 18) with a conserved HH, including a shared segment from marker rs7703994 to marker rs879143 (GRCh37/hg19 chr5:3339142-10620274) that

overlaps partially with the MCDR3 locus. No rare exonic variants were detected within this interval.

Discussion

This report describes a novel phenotype consisting of characteristic yellow dots at the macula, which are first evident in childhood and are usually associated with good visual function. The condition is commonly sporadic, although it may also segregate in an autosomal dominant manner.

Most of the affected individuals were female. The macular abnormalities were identified as an incidental finding on routine funduscopy in the majority of subjects, or were discovered during examination of the family members of affected individuals. The condition appears to be non-progressive and, in familial cases, the macular appearance was similar in children and older adults, suggesting that the disorder is stationary. The phenotype is associated with normal visual acuity and normal color vision in the majority of affected individuals. The full-field ERG showed no evidence of generalised retinal dysfunction in any subject, although in one subject the PERG indicated moderate macular dysfunction and in another, very mild macular dysfunction. Overall the normal visual acuity, color vision and retinal electrophysiology are consistent with normal macular function, although it is possible that more detailed psychophysical testing, for example microperimetry, may have revealed subtle loss of retinal sensitivity. OCT of the central retina showed normal retinal thickness and, in the majority, a normal ISe band, in keeping with the good visual acuity. In a small minority there were subtle irregularities at the ISe band outside the fovea.

Many different inherited disorders are associated with 'deposits' at the macula. However, they may be distinguished from the phenotype described here by the age of onset, associated visual loss, disease progression, retinal electrophysiology and results of OCT imaging. A similar non-progressive retinal phenotype with drusenoid deposits that are present from childhood can be seen in North Carolina Macular Dystrophy (NCMD), a dominantly inherited macular dystrophy which has been mapped to chromosome 6q16 (MCDR1 locus) [15]. The ERG and EOG are also normal in NCMD, with dysfunction being confined to the macula. Recently, Small *et al.* identified rare variants upstream of the retinal transcription factor gene

PRDM13 in families with NCMD that link to the MCDR1 locus [14]. An identical phenotype has been mapped to chromosome 5p15 (MCDR3 locus) [16], [17]. Although the disorder reported here is also of early onset, is non-progressive and is associated with a normal ERG and EOG, there are a number of differences between the two. There may be considerable phenotypic heterogeneity in NCMD, with some family members having normal visual acuity with drusen-like deposits, whilst others have large ectatic macular lesions causing central visual loss. Furthermore, there is generally a family history consistent with an autosomal dominant inheritance pattern. Most of the present cases were sporadic or from small families. Those family members of sporadic cases who were examined had normal fundi. WES in 7 subjects failed to reveal any mutations in known retinal dystrophy genes, and SNP-based haplotype sharing analysis excluded linkage to the MCDR1 locus and a portion of the MCDR3 locus, adding support to the hypothesis that this is a new macular condition. Further molecular analysis is required to determine the etiology.

Drusen-like deposits at the macula may be seen in children and young adults in a variety of ocular and syndromic disorders (for review see Khan *et al* 2016) [18]. Small yellow deposits may be present in the early stages of the macular dystrophy associated with mutations in *PRPH2*, but the macular abnormalities, which are rarely seen before teenage years, are progressive and are often associated with full-field ERG abnormalities, particularly in late disease [19, 20]. Macular drusen are seen in autosomal dominant drusen but again, those have a later age of onset, a different retinal distribution and a different appearance on retinal imaging [21-23]. Drusen-like deposits at the macula have also been reported in systemic disorders such as mesangioproliferative glomerulonephritis type 2 and lipodystrophy, but in those disorders the drusen are larger, more extensive and increase in number with age [24]-[25, 26]. Similar macular deposits have been reported in association with other systemic findings in individuals with ring chromosome 17 and trisomy 10q [27-30]. However, none of the present subjects had any relevant systemic abnormalities.

The affected individuals in the present study were identified at routine optometric visits or by examination of other affected family members. Visual acuity was normal in the majority, and

in all but one subject this was accompanied by normal electroretinographic findings that investigated both the detailed macular function (PERG) and global retinal function (ERG). Although no significant longitudinal data are available, none of the subjects showed progression over time, and the similarity of fundus appearance across generations in familial cases suggests the phenotype to be non-progressive.

The novel macular phenotype described here has a characteristic appearance on fundus examination and retinal imaging. However in order to exclude other disorders with a similar appearance early in the disease process, it is important to demonstrate normal retinal function. Investigations should include a full-field ERG and pattern ERG or multifocal ERG. OCT is also useful to exclude other phenotypes with drusen-like deposits [18]. The major differential diagnosis is from NCMD, where there is also a normal ERG, but examination of other family members should allow this disorder to be excluded.

To conclude, a novel childhood onset macular phenotype is described in which there are multiple yellow dots at the macula associated with normal macular function. The condition is of early onset and may be developmental in origin; it appears to be distinct from other developmental macular dystrophies. The yellow dots are hyperautofluorescent on FAF imaging and may show subtle irregularities at the inner segment ellipsoid band on OCT imaging. Such a phenotype has not, to our knowledge, been previously reported. Affected individuals can be reassured that the condition is benign and unlikely to be associated with any significant visual loss.

References

1. Moore, A.T., *Childhood macular dystrophies*. Current opinion in ophthalmology, 2009. **20**(5): p. 363-8.
2. North, V., R. Gelman, and S.H. Tsang, *Juvenile-onset macular degeneration and allied disorders*. Dev Ophthalmol, 2014. **53**: p. 44-52.
3. Michaelides, M., D.M. Hunt, and A.T. Moore, *The genetics of inherited macular dystrophies*. Journal of medical genetics, 2003. **40**(9): p. 641-50.
4. Michaelides, M., G. Jeffery, and A.T. Moore, *Developmental macular disorders: phenotypes and underlying molecular genetic basis*. Br J Ophthalmol, 2012. **96**(7): p. 917-24.
5. O'Sullivan, J., et al., *A paradigm shift in the delivery of services for diagnosis of inherited retinal disease*. Journal of medical genetics, 2012. **49**(5): p. 322-6.
6. Marmor, M.F., et al., *ISCEV Standard for full-field clinical electroretinography (2008 update)*. Documenta ophthalmologica. Advances in ophthalmology, 2009. **118**(1): p. 69-77.
7. Holder, G.E., et al., *ISCEV standard for clinical pattern electroretinography--2007 update*. Documenta ophthalmologica. Advances in ophthalmology, 2007. **114**(3): p. 111-6.
8. Brown, M., et al., *ISCEV Standard for Clinical Electro-oculography (EOG) 2006*. Documenta ophthalmologica. Advances in ophthalmology, 2006. **113**(3): p. 205-12.
9. Hufnagel, R.B., et al., *Neuropathy target esterase impairments cause Oliver-McFarlane and Laurence-Moon syndromes*. J Med Genet, 2015. **52**(2): p. 85-94.
10. DePristo, M.A., et al., *A framework for variation discovery and genotyping using next-generation DNA sequencing data*. Nat Genet, 2011. **43**(5): p. 491-8.
11. Li, H. and R. Durbin, *Fast and accurate short read alignment with Burrows-Wheeler transform*. Bioinformatics, 2009. **25**(14): p. 1754-60.
12. Miyazawa, H., et al., *Homozygosity haplotype allows a genomewide search for the autosomal segments shared among patients*. Am J Hum Genet, 2007. **80**(6): p. 1090-102.
13. Bowne, S.J., et al., *North Carolina macular dystrophy (MCDR1) caused by a novel tandem duplication of the PRDM13 gene*. Mol Vis, 2016. **22**: p. 1239-1247.
14. Small, K.W., et al., *North Carolina Macular Dystrophy Is Caused by Dysregulation of the Retinal Transcription Factor PRDM13*. Ophthalmology, 2016. **123**(1): p. 9-18.
15. Small, K.W., *North Carolina macular dystrophy: clinical features, genealogy, and genetic linkage analysis*. Trans Am Ophthalmol Soc, 1998. **96**: p. 925-61.
16. Rosenberg, T., et al., *Clinical and genetic characterization of a Danish family with North Carolina macular dystrophy*. Mol Vis, 2010. **16**: p. 2659-68.
17. Michaelides, M., et al., *An early-onset autosomal dominant macular dystrophy (MCDR3) resembling North Carolina macular dystrophy maps to chromosome 5*. Investigative ophthalmology & visual science, 2003. **44**(5): p. 2178-83.
18. Khan, K.N., et al., *Differentiating drusen: Drusen and drusen-like appearances associated with ageing, age-related macular degeneration, inherited eye disease and other pathological processes*. Prog Retin Eye Res, 2016. **53**: p. 70-106.
19. Piguet, B., et al., *Full characterization of the maculopathy associated with an Arg-172-Trp mutation in the RDS/peripherin gene*. Ophthalmic Genet, 1996. **17**(4): p. 175-86.
20. Boon, C.J., et al., *The spectrum of retinal dystrophies caused by mutations in the peripherin/RDS gene*. Prog Retin Eye Res, 2008. **27**(2): p. 213-35.
21. Holz, F.G., et al., *Ultrastructural findings in autosomal dominant drusen*. Arch Ophthalmol, 1997. **115**(6): p. 788-92.
22. Edwards, A.O., et al., *Malattia leventinese: refinement of the genetic locus and phenotypic variability in autosomal dominant macular drusen*. Am J Ophthalmol, 1998. **126**(3): p. 417-24.
23. Zweifel, S.A., et al., *Multimodal imaging of autosomal dominant drusen*. Klin Monbl Augenheilkd, 2012. **229**(4): p. 399-402.
24. D'Souza, Y., et al., *Long-term follow-up of drusen-like lesions in patients with type II mesangiocapillary glomerulonephritis*. Br J Ophthalmol, 2008. **92**(7): p. 950-3.

25. Duvall-Young, J., M.K. MacDonald, and N.M. McKechnie, *Fundus changes in (type II) mesangiocapillary glomerulonephritis simulating drusen: a histopathological report*. Br J Ophthalmol, 1989. **73**(4): p. 297-302.
26. Davis, T.M., et al., *Retinal pigment epithelial change and partial lipodystrophy*. Postgrad Med J, 1988. **64**(757): p. 871-4.
27. Charles, S.J., et al., *Flecked retina associated with ring 17 chromosome*. Br J Ophthalmol, 1991. **75**(2): p. 125-7.
28. Gass, J.D. and B.S. Taney, *Flecked retina associated with cafe au lait spots, microcephaly, epilepsy, short stature, and ring 17 chromosome*. Arch Ophthalmol, 1994. **112**(6): p. 738-9.
29. Neely, K., et al., *Ocular findings in partial trisomy 10q syndrome*. Am J Ophthalmol, 1988. **106**(1): p. 82-7.
30. Tabandeh, H., et al., *Drusen-like macular deposits in partial trisomy 10q*. Retina, 2000. **20**(6): p. 678-9.

Table Titles

Table 1. Clinical features of Benign Yellow Dot Maculopathy Subjects

Table 2. Fundus features in Benign Yellow Dot Maculopathy

Supplementary Table 1. Homozygosity Haplotype analysis of Family 4

Figure Titles

Figure 1. Pedigrees of Families 4, 8 and 22 that underwent molecular analysis

Figure 2. Fundus images of Benign Yellow Dot Maculopathy Subjects

Figure 3. Fundus autofluorescence of Benign Yellow Dot Maculopathy Subjects

Figure 4. OCT images of Benign Yellow Dot Maculopathy Subjects

Supplementary Figure 1. Identification of the candidate regions for Family 4 (GC14302) using the Homozygosity Haplotype approach

Table Legends

Table 1.

Key: GC number – Genetics Clinic number (Subjects recruited from Moorfields Eye Hospital, UK); BCVA – Best Corrected Visual Acuity; RE – Right Eye; LE – Left Eye; F – Female; FH – Family History; G.mother – Grandmother; M – Male; Hypermet – Hypermetropia; ET – Esotropia; Strab – Strabismus; Unr – Unrecorded; Bilat – Bilateral

Table 2.

Key: RE – Right eye

Figure Legends

Figure 1.

Family 4 had 5 affected individuals in two successive generations; Family 8 had 2 affected individuals in two successive generations; Family 22 had only one affected individual. Black circles / squares denote affected individuals

Figure 2.

A – Familial benign yellow dot maculopathy, Subject 11; B – Sporadic benign yellow dot maculopathy, fine, discrete, dots, Subject 24; C – Sporadic benign yellow dot maculopathy, concentrated in the nasal parafoveal region, Subject 26; D – Sporadic benign yellow dot maculopathy, confluent, Subject 28; E - Sporadic benign yellow dot maculopathy, Subject 34; F – Familial benign yellow dot maculopathy, Subject 19

Figure 3.

The yellow dots show hyperautofluorescence on fundus autofluorescence imaging.

A –Subject 11; B –Subject 24; C –Subject 26; D – Subject 28; E – Subject 34; F – Subject 19

Figure 4.

A – Normal OCT, Subject 24; B – Slight irregularity of the inner segment ellipsoid band, indicated by the arrow, Subject 26; C – Slight irregularity of the RPE layer, indicated by the arrow, Subject 11. Arrows correspond to the location of the dots as identified from the infra-red reflectance images obtained during fundus autofluorescence image acquisition

Supplementary Figure 1.

Five affected family members with SNP chip data were included in the analysis. A densitogram of the genomic Regions with a Conserved Homozygosity Haplotype (RCHHs) is depicted. The darker the color, the more individuals share a HH in the region. Black regions indicate RCHHs that are shared by all 5 affected family members included in the analysis

Table 1.

Subject no, Family no (GC number)	Proband?	Presenting age (years)	Gender	Mode of Presentation	Family history	BCVA LogMAR RE, LE (Age, years)	Past Ocular History
1, 1	Proband	5	F	Community	Dominant	0, 0 (5)	Nil
2, 1	Mother	28	F	FH	Dominant	0, -0.08 (28)	Nil
3, 1	Maternal G.mother	50	F	FH	Dominant	-0.08, -0.08 (50)	Nil
4, 2	Proband	14	M	Community	Dominant	-0.08, 0 (14)	Hypermet, ET, strab surgery
5, 2	Mother	43	F	FH	Dominant	0.18, 0.18 (43)	Refractive error
6, 3	Proband	45	F	Community	Dominant	-0.08, -0.08 (45)	Nil
7, 3	Son	6	M	FH	Dominant	-0.08, -0.08 (6)	Nil
8, 4 (GC14302)	Proband	15	F	Community	Dominant	0.78, 0.78 (15)	Non organic visual loss
9, 4 (GC14302)	Sister	18	F	Community	Dominant	0, 0, (18)	Nil
10, 4 (GC14302)	Mother	45	F	FH	Dominant	0.18, 0.18 (45)	Refractive error
11, 4 (GC14302)	Maternal 1st cousin	10	M	FH	Dominant	-0.08, -0.08 (10)	Nil
12, 5 (GC16206)	Proband	22	F	Community	Dominant	-0.08, -0.08 (22)	Refractive error
13, 5 (GC16206)	Mother	Unr	F	FH	Dominant	0, 0, (Unr)	Nil
14, 6	Proband	7	F	Community	Dominant	0, 0 (7)	Nil
15, 6	Father	Unr	M	FH	Dominant	Unr, Unr (Unr)	Nil
16, 6	Paternal G.mother	59	F	FH	Dominant	Unr, Unr (Unr)	Nil
17, 7	Proband	11	F	Community	Dominant	0, 0 (11)	Refractive error
18, 7	Father	Unr	M	FH	Dominant	Unr, Unr (Unr)	Nil

19, 8	Proband	7	F	Community	Dominant	0, 0 (7)	Refractive error
20, 8	Mother	45	F	FH	Dominant	0, 0 (45)	Nil
21, 8	Brother	13	M	FH	Dominant	0, 0 (13)	Nil
22, 9	Proband	8	F	Community	Sporadic	0, 0 (8)	Nil
23, 10 (GC17650)	Proband	6	M	Another Ophthalmologist	Sporadic	0.7, 0.8 (6)	Hypermet, ET, bilat Ametropic amblyopia
24, 11 (GC19048)	Proband	10	F	Community	Sporadic	0, 0 (10)	Refractive error
25, 12 (GC19084)	Proband	5	F	Community	Sporadic	0, 0 (10)	Bilateral optic neuropathy
26, 13	Proband	10	F	Community	Sporadic	0, 0 (10)	Nil
27, 14	Proband	12	F	Community	Sporadic	0.4, 0 (14)	Hypermet, Anisometropic amblyopia
28, 15	Proband	14	M	Community	Sporadic	0.08, 0.14 (14)	Hypermet, Ametropic amblyopia
29, 16 (GC17091)	Proband	15	F	Community	Sporadic	0, 0 (15)	Refractive error
30, 17	Proband	15	M	Community	Sporadic	0, 0 (15)	Nil
31, 18 (GC18107)	Proband	28	M	Community	Sporadic	0, 0 (29)	Nil
32, 19	Proband	28	F	Community	Sporadic	-0.08, -0.08 (29)	Refractive error
33, 20	Proband	29	F	Community	Sporadic	0, 0 (29)	Refractive error
34, 21	Proband	8	F	Community	Sporadic	0, 0 (8)	Refractive error
35, 22	Proband	16	F	Community	Sporadic	0, 0 (16)	Nil
36, 23	Proband	5.5	F	Community	Sporadic	0, 0 (5.5)	Refractive error

Table 2.

Subject no, Family no	Macula		Optic disc
1, 1	Discrete, Fine, Yellow dots	Concentrated in temporal parafovea	Fine yellow crescent around temporal border of disc
2, 1	Discrete, Fine, Yellow dots		
3, 1	Discrete, Fine, Yellow dots		
4, 2	Discrete, Fine, Yellow dots	Concentrated in nasal parafovea	
5, 2	Discrete, Fine, Yellow dots		
6, 3	Discrete, Fine, Yellow dots		
7, 3	Discrete, Fine, Yellow dots		
8, 4	Discrete, Yellow dots, Variable sizes, Some confluent	Even distribution	Yellow crescent around nasal border of disc between 12-6 o'clock
9, 4	Discrete, Fine, Yellow dots	Even distribution	Yellow crescent around disc 360 degrees
10, 4	Discrete, Yellow dots, Larger	Even distribution	Yellow crescent around temporal border of disc between 12-6 o'clock
11, 4	Discrete, Yellow dots, Variable sizes, Some confluent	Even distribution	Yellow crescent around disc 360 degrees
12, 5	Discrete, Fine, Yellow dots	Concentrated in nasal parafovea	Yellow crescent around disc temporally
13, 5	Discrete, Yellow dots, Variable sizes, Some confluent	Concentrated in nasal parafovea	Yellow crescent around disc 360 degrees
14, 6	Discrete, Yellow dots, Variable sizes, Some confluent	Concentrated in superior parafovea	Yellow crescent around disc temporally - left eye
15, 6	Discrete, Fine, Yellow dots	Concentrated in superior parafovea	Yellow crescent around nasal border of disc between 12-6 o'clock
16, 6	Discrete, Fine, Yellow dots, Some confluent	Concentrated in superior parafovea	Peri-papillary atrophy
17, 7	Discrete, Fine, Yellow dots, Some confluent	Even distribution	Halo around disc resembling peri-papillary atrophy
18, 7	Discrete, Fine, Yellow dots	Concentrated in nasal parafovea	Yellow crescent around disc 360 degrees
19, 8	Discrete, Fine, Yellow dots	Concentrated in nasal parafovea	Yellow crescent around disc 360 degrees

20, 8	Discrete, Fine, Yellow dots	Concentrated in nasal parafovea	Not visible
21, 8	Discrete, Fine, Yellow dots	Concentrated in nasal parafovea	Not visible
22, 9	Discrete, Yellow dots, Variable sizes, Some confluent	Even distribution, some extra-macula in RE	Yellow crescent around disc 360 degrees
23, 10	Discrete, Fine, Yellow dots	Even distribution	No crescent
24, 11	Discrete, Fine, Yellow dots	Even distribution, some extra-macula in RE	Yellow crescent around disc 360 degrees
25, 12	Discrete, Fine, Yellow dots	Even distribution	Yellow crescent around disc 360 degrees
26, 13	Discrete, Fine, Yellow dots	Concentrated in nasal parafovea	Yellow crescent around disc temporally; full discs - no swelling
27, 14	Discrete, Fine, Yellow dots	Concentrated in nasal parafovea	Yellow crescent around disc 360 degrees
28, 15	Discrete, Yellow dots, Many confluent	Concentrated in nasal parafovea	Halo around disc resembling peri-papillary atrophy
29, 16	Discrete, Fine, Yellow dots	Even distribution	Halo around disc, temporally
30, 17	Discrete, Fine, Yellow dots	Concentrated in nasal parafovea	Peri-papillary atrophy temporal
31, 18	Discrete, Yellow dots, Variable sizes, Some confluent	Concentrated in nasal parafovea	Yellow crescent around disc, temporally
32, 19	Discrete, Fine, Yellow dots	Even distribution	Yellow crescent around disc 360 degrees
33, 20	Discrete, Fine, Yellow dots	Even distribution	Peri-papillary atrophy
34, 21	Discrete, Fine, Yellow dots	Even distribution	Yellow crescent around disc 360 degrees
35, 22	Discrete, Fine, Yellow dots	Concentrated in nasal parafovea	Not visible
36, 23	Discrete, Fine, Yellow dots	Concentrated in temporal parafovea RE	Not visible

Supplementary Table 1.**Homozygosity Haplotype analysis of Family 4**

Chromosome	Physical position (bp)	start/end	SNP	Genetic distance (cM)
2	206652963	start	rs3755232	213.82
2	216770807	end	rs11891588	223.84
3	61495	start	rs13060385	0.00
3	8808285	end	rs237897	22.56
3	30590213	start	rs7616969	53.38
3	31757599	end	rs3792549	54.80
5	3339142	start	rs7703994	8.37
5	10620274	end	rs879143	24.55
6	80454831	start	rs2092745	89.15
6	91531693	end	rs9351245	97.75
8	33203726	start	rs1996363	61.52
8	39850058	end	rs2543073	66.32
8	96979871	start	rs10955055	107.65
8	123931864	end	rs16897667	131.52
11	69269768	start	rs7113550	74.86
11	81842796	end	rs1892876	89.55
17	57480798	start	rs7213065	83.10
17	67336421	end	rs17687227	95.08
18	27500959	start	rs9304548	49.08
18	78015180	end	rs12960632	117.71

Figure 1

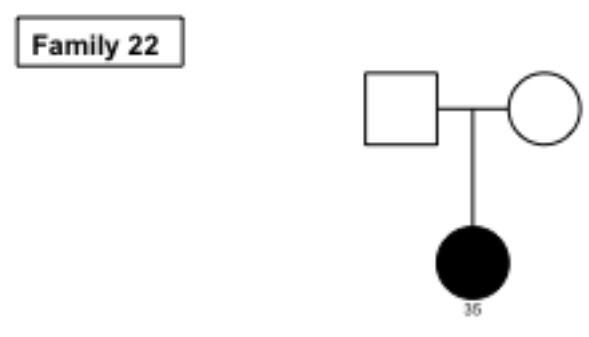
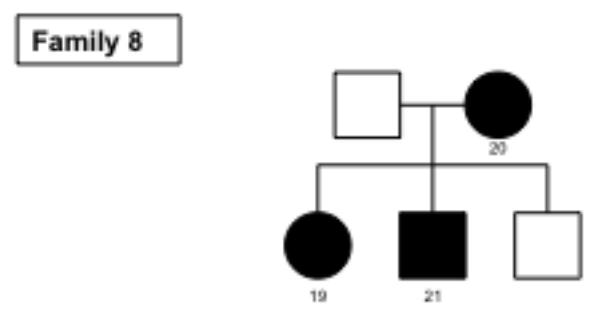
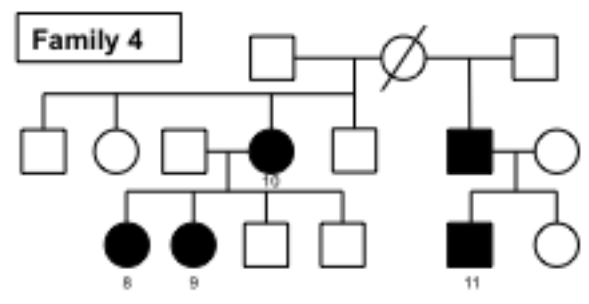


Figure 2

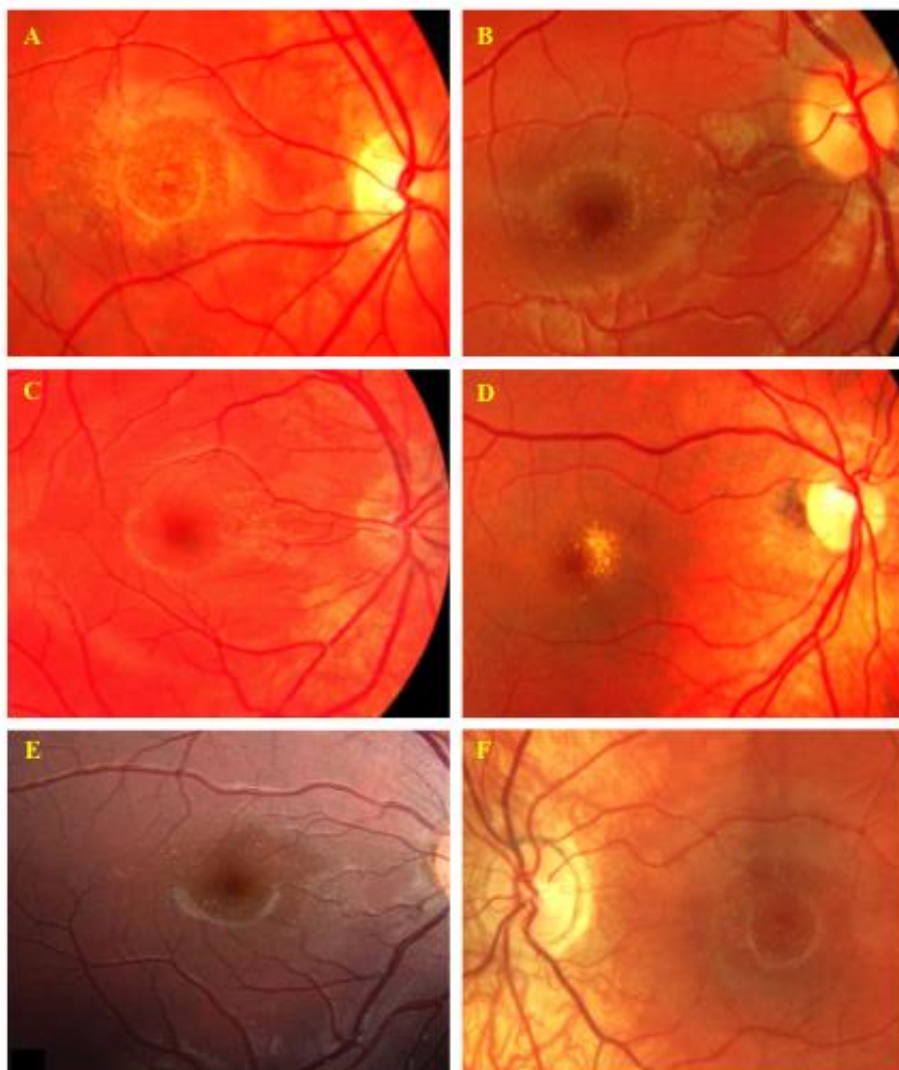


Figure 3

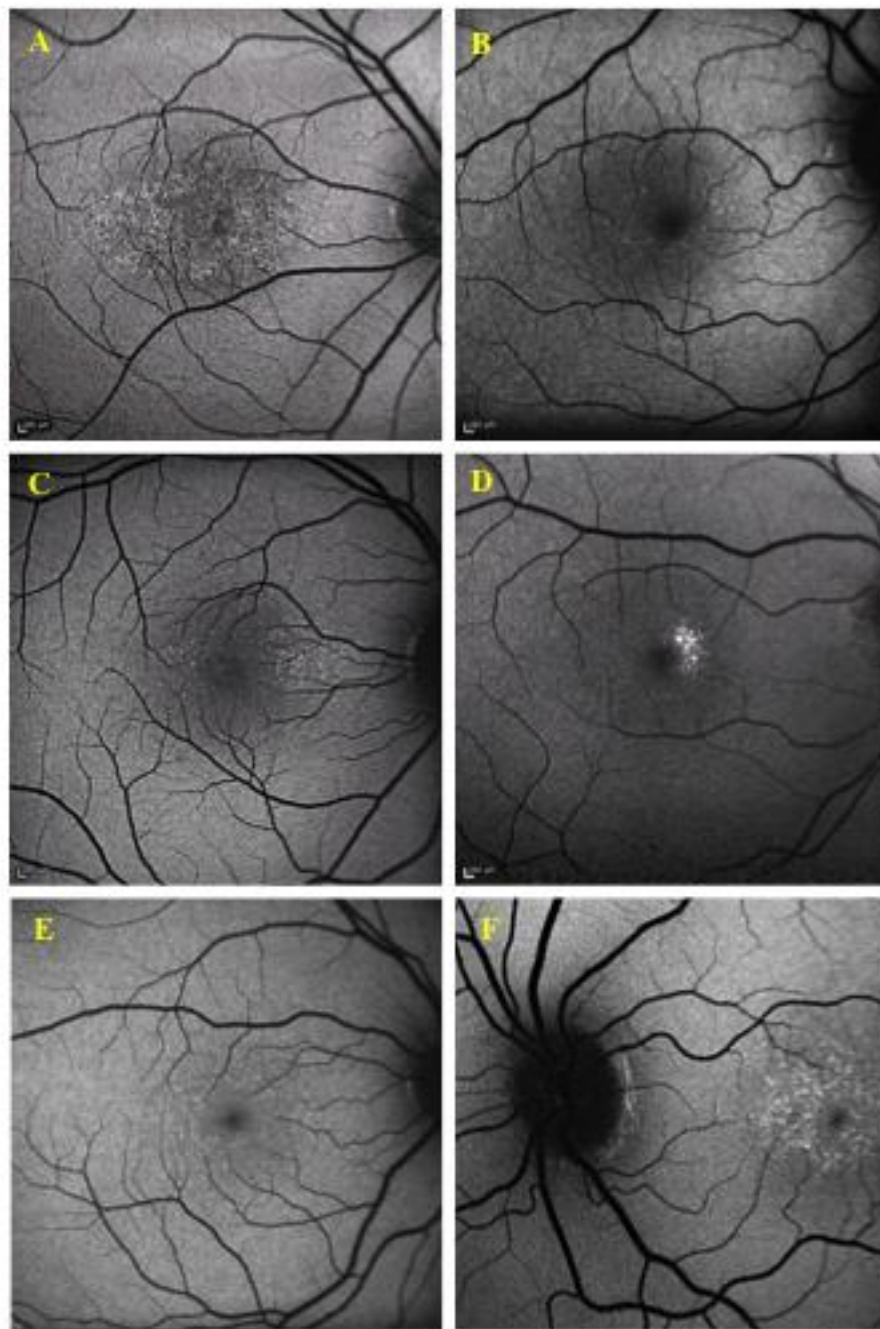
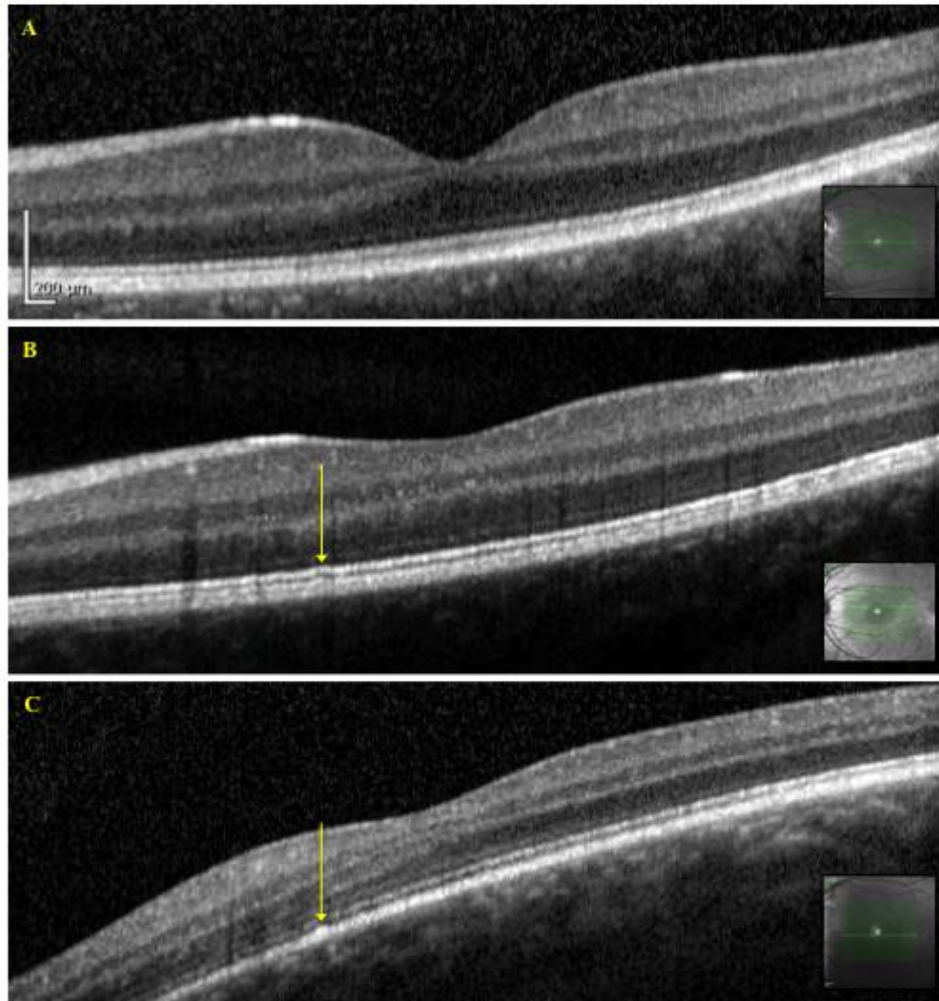


Figure 4



Supplementary Figure 1.

